Role of very-high-frequency excitation in single-bubble sonoluminescence

Francisco J. Moraga,[1,*] Rusi P. Taleyarkhan,[2] Richard T. Lahey, Jr.,[3] and Fabian J. Bonetto[4]
[1]*Oak Ridge Associated Universities, Oak Ridge, Tennessee 37831*
[2]*Oak Ridge National Laboratory, Oak Ridge, Tennessee 37831*
[3]*Rensselaer Polytechnic Institute, Troy, New York 12180*
[4]*Instituto Balseiro/CNEA-CAB. Bariloche, Argentina*
(Received 20 December 1999)

The fundamental and tenth harmonics were used to produce stable single-bubble sonoluminescence in water. By varying the phase difference between the harmonics, it was possible to enhance the sonoluminescence light emission by as much as a factor of 2.7 compared with single-frequency excitation. Absolute measurements of the bubble radius evolution were carried out using the two-detector technique. Unlike previous observations, these measurements and complementary fits of the Rayleigh-Plesset equation reveal that the maximum bubble radius does not change significantly with phase angle between the harmonics. Therefore, increased sonoluminescence intensity does not have to correlate with increases in maximum bubble radius prior to collapse. We believe that a more violent bubble collapse rate (driven by the very-high-frequency component) is responsible for the enhanced light emission under this type of mixed excitation. It was further found that the presence of the tenth-harmonic frequency component led to significant enhancements in the stability of the bubble undergoing sonoluminescence. This allowed the bubble to be driven at the fundamental frequency at 2.0 bars pressure amplitudes, which are significantly above often-reported thresholds of 1.4 bar itself, thereby leading to increased levels of light emission (by more than 250%).

PACS number(s): 78.60.Mq, 42.65.Re, 43.25.+y

INTRODUCTION

The motivation of this experiment is to achieve more violent bubble compressions than what is generally achieved in single-bubble sonoluminescence. In order to achieve more violent compressions, one can generate a low pressure at the bubble location at the moment the bubble is at its maximum radius or generate a high pressure at the bubble location at the moment the bubble is collapsing. The latter strategy was selected for this experiment. We used a very-high-frequency standing pressure wave, the highest frequency ever reported in the literature, to compress the bubble more violently during the collapse. We believe that a pressure oscillation of duration comparable to that of the bubble collapse should be used. During the rest of the cycle, the bubble dynamics and the levitation position are determined mainly by pressure oscillations at the fundamental frequency of the chamber.

Recently, other researchers [1–3] experimentally used the first harmonics of their resonator to excite the bubble with two frequencies. In both cases they obtained an increase in the sonoluminescence (SL) light intensity. Delgadino *et al.* [2,3] measured a factor of 2 increase in SL intensity, while Holzfuss *et al.* [1] measured a maximum factor of 3. Delgadino *et al.* measured an increase in the ratio between the maximum and ambient bubble radius, while Holzfuss *et al.* expected such an increase from numerical calculations based on the Rayleigh-Plesset equation. In contrast, our high-frequency driving scheme aims to intensify the violence of the collapse via minimizing the minimum bubble radius for a given maximum radius prior to collapse.

*Present address: Rensselaer Polytechnic Institute, Troy, NY 12180.

SETUP DESCRIPTION

The resonator was a 65-mm-o.d. glass sphere custom blown to be of spherical shape. The neck of the chamber, located at the North Pole, was made to accept a stopper of size 00. Two pairs of disk-shaped piezoelectric ceramic transducers were cemented with epoxy at the equatorial plane of the resonator. One pair was used to produce the standing wave at the fundamental mode of the chamber ($f_0 = 27.1245$ kHz), while the other pair provided excitation at $10f_0$. Each pair consisted of two transducers at opposite sides of an equatorial diameter, with any given transducer at 90° of its two neighbors. A piezoelectric ceramic disk of 3 mm o.d. was glued at the South Pole. It acted as a microphone. The experiments were conducted in water at 16 °C in a chamber open to the atmosphere. The chamber was suspended from its neck and was mounted on a three-dimensional (3D) traversing mechanism.

The power electronics for the low-frequency driving consists of a function generator (Hewlett-Packard 33120A) with 2 ppm stability, a low-frequency amplifier, and a resonant *RLC* circuit where the capacitance is that of the ceramic transducers. A typical root-mean-square voltage at the low-frequency piezoceramic transducers was 186 V. The high-frequency power electronics consisted of another function generator (Hewlett-Packard 33120A) and a linear amplifier (Piezo Systems, Inc., part No. EPA-102-115). This high-frequency amplifier has a 0.3-MHz bandwidth and a maximum power output of 40 W. The two wave generators were always phase locked. The 2-ppm stability assured us a controllable phase difference between the two frequencies. The high frequency has to be an integer multiple of the low frequency. This requisite assures us that phase difference is a meaningful term. We could have relaxed this requisite to

have the frequency ratio to be a fractional number. This fractional number should be a ratio between two small integers. The factor of 10 between the two frequencies was chosen after verifying that the chamber could produce standing waves at that frequency and that the quality factor of the chamber was comparable or better to that of other integer multiples of f_0 in the neighborhood of 10.

A Precision Acoustics needle hydrophone was used to measure the acoustic pressure at the center of the resonator and to make sure that standing waves were produced. Additionally, we used the needle hydrophone positioned at the center of the chamber to make sure that both harmonics could be excited independently within the amplitude range used. The Fourier transform of the pressure signals at the center of the chamber for single- and multiple-frequency excitation showed that there is no bleeding of energy from the fundamental to higher harmonics and that the pressure amplitude at the fundamental frequency was independent of the high-frequency driving voltage. The diameter of the hydrophone tip is 2 mm. The sensor at the tip is a polyvinylidene difluoride disk of 1 mm diameter and 28 μm thick. Although this sensor is small enough to measure standing waves at the fundamental frequency, care should be taken interpreting the measurements of the hydrophone at $10f_0$ because of the inherent directionality and spatial averaging characteristics of a 1-mm aperture. Because of this reason, the voltage at the high-frequency piezoceramic transducers was also used to characterize the high-frequency pressure amplitude.

A helium-neon (He-Ne) laser was used to illuminate the bubble. At 80° in the forward-scattering direction, a lens was used to collect light in a 27° angle. This light was collimated on a Hamamatsu R212 photomultiplier. The photomultiplier signal was sent to a 5-MHz bandwidth preamplifier (Hamamatsu C1053-51). When the laser was on, the photomultiplier signal was used to measure the bubble radius. When it was off, the photomultiplier recorded the bubble light emission. The bubble radius R is obtained from the measured voltages V at the output of the photomultiplier preamplifier as $R=R_m[(V-V_n)/V_m]^{1/2}$, where $V_n=3$ mV is the noise level, $V_m \gg V_n$ is the maximum measured voltage, and R_m is the maximum bubble radius. This relationship assumes that the intensity of laser light scattered by the bubble is proportional to R^2. This hypothesis is known to hold at the Brewster angle, particularly for large collecting solid angles [2,4], and is valid for our experimental setup. It must be observed that the maximum radius R_m cannot be determined from the photomultiplier tube (PMT) measurements without making a fit with the Rayleigh-Plesset equation. In order to provide a direct absolute measurement of the bubble radius, an avalanche photodiode (APD) was also used to monitor the laser light scattered by the bubble. The APD was located at 34° in the forward-scattering direction, at 185 mm from the chamber center, and has a 10-mm-diam circular sensitive area. As the bubble radius increases, relative maxima and minima of the light intensity collected by the APD arise. The change of radius between two consecutive maxima can be calculated using Mie theory [5]. Counting the maxima that occur during bubble expansion provides the additional information necessary to produce absolute numbers for the bubble radius directly from the measurements. An additional advantage of this so-called two-detector technique originally developed by Delgadino [2] is that results are independent of the light intensity and of the bubble position in the laser beam.

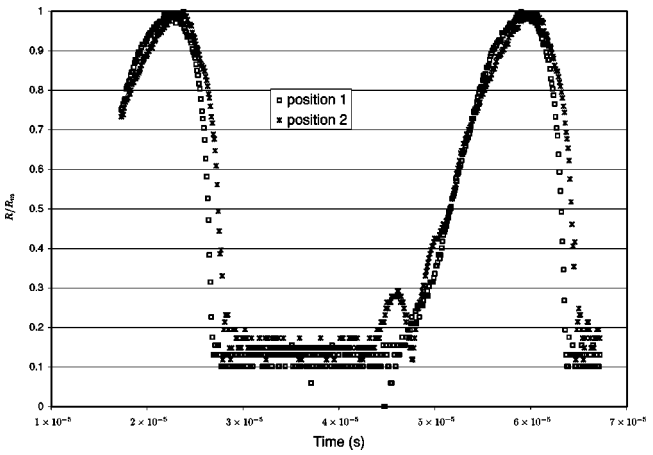

FIG. 1. Normalized bubble radius for two different bubble positions. Phase angle between wave generators $=-0.8°$.

EXPERIMENTAL METHOD

In a resonator open to the atmosphere, the concentration of dissolved air increases with time until the saturation level is reached. This variation can significantly impact the SL light intensity [4]. Our experimental method was based on making sure that the changes in the SL light intensity were due to the dual-frequency driving scheme employed and not to variations in the dissolved gas concentration. The concentration of gas dissolved in the water was measured with a dissolved oxygen meter (YSI Inc., model 55). Measured values for the gas concentration at the beginning and end of a run of 1 h, 15 min duration are 1.77 mg/l (18% at 16 °C) and 2.60 mg/l (27% at 16 °C), respectively. The probe of the oxygen meter does not fit into the chamber. Thus the measurements were made in another container. Since some air will be dissolved when moving the water between containers, the 18% and 27% measurements are an under- and overestimation, respectively. Stable single-bubble sonoluminescence has been observed for air concentrations of up to 50% [6]. In order to avoid a temperature transient, the degassed water was cooled down to the chamber temperature before introducing it in the chamber.

We only considered data sets in which either the high-frequency amplitude or the phase between frequencies was varied parametrically and in a time scale in the order of a few minutes to an hour. It is important to stress that an $x°$ change of phase between wave generators corresponds to an $x°$ change of phase between the low- and high-frequency pressure waves at the bubble location, only if the bubble position remains the same. For this reason all data presented in this work are for very low amplitudes of the high-frequency signal, since at larger amplitudes the bubble position changed when the wave generators phase angle was varied. Figure 1 shows the bubble radius time evolution for two bubble positions, estimated to be 3 mm apart. The phase angle between wave generators is $-0.8°$ in both cases. At position 2 (see Fig. 1), the bubble experiences a small expansion and contraction right before the main expansion. This small expan-

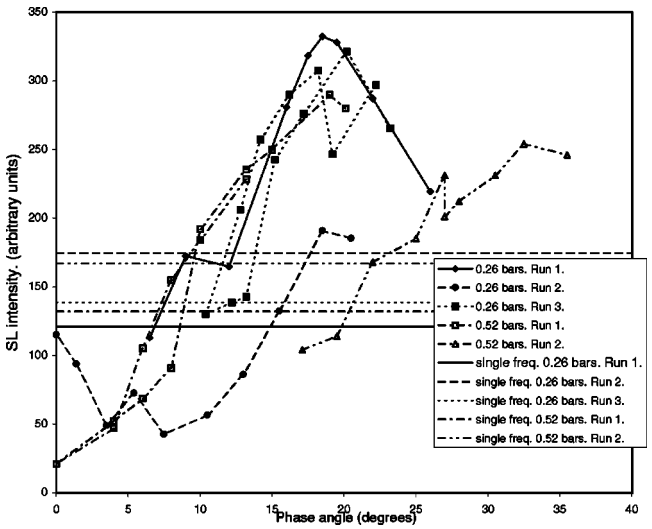

FIG. 2. SL intensity as a function of phase angle for two high-frequency pressure amplitudes. Low-frequency pressure amplitude $=1.50$ bars.

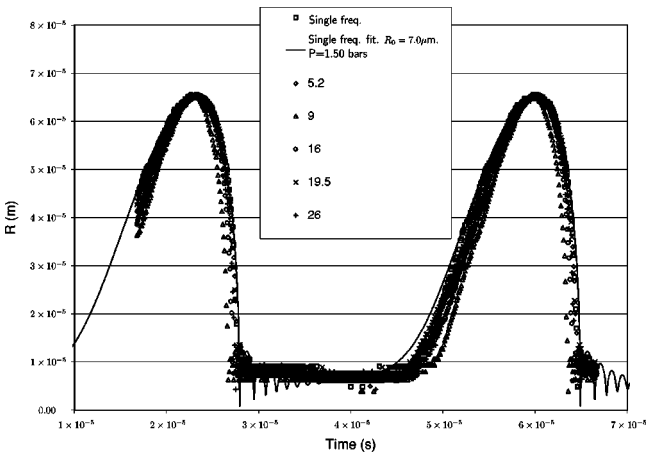

FIG. 3. Bubble radius vs time for different phase angles (run 1 at 0.26 bar in Fig. 2). High-frequency pressure amplitude $=0.26$ bars.

sion and contraction is absent at position 1 (see Fig. 1). It is evident from Fig. 1 that the bubble radius evolution depends on the bubble position. Thus, in order to correlate SL intensities with phase angle between wave generators, it is convenient to consider only data for a fixed bubble position. The helium-neon laser was used to make sure the bubble position was fixed. In a few selected runs, we used two crossing laser beams to completely identify the position of the bubble.

Comparisons between the SL intensity for single- and double-frequency excitation are made using the single-frequency intensity measured immediately before and/or after the double-frequency excitation data and for the same bubble. Moreover, in order to avoid changes of bubble positions when the high-frequency driving was turned on (off), a potentiometer was used to change continuously the high-frequency driving from (to) a small value that could not be detected by the needle hydrophone to (from) the target value. At every other point, the laser was used to verify that the bubble did not move and that the bubble image was fully inside the sensitive area of the photomultiplier.

RESULTS

Figure 2 shows the sonoluminescence light intensity versus the phase angle between wave generators. A phase change of 36° corresponds to a complete cycle of the high frequency. It must be noticed that the actual phase angle between the high- and low-frequency pressure waves at the bubble location depends on the bubble position. Each run in Fig. 2 corresponds to a bubble at a fixed position. The position uncertainty is that of the beam thickness. The nominal beam diameter at e^{-2} intensity is 0.7 mm. In contrast, the wavelength corresponding to $10f_0$ is 5.5 mm. Because the bubble position changed from one run to the next, it is *meaningless* to compare phase angles between different runs. However, since the bubble did not move during any given run, an $x°$ phase change between wave generators in a given run corresponds to an $x°$ phase change between the pressure waves at the bubble location. A relatively smooth and continuous variation of the SL intensity with the phase angle is observed, strongly indicating that the phase angle is a parameter very important in determining the SL intensity. Three runs at 0.26-bar and two runs at 0.52-bar high-frequency pressure amplitudes can be seen in the figure (0.64 and 1.29 V root mean square, respectively, at the high-frequency transducers). The lines indicate the chronological order in which the data points were acquired. Thus run 3 at 0.26 bar and run 1 at 0.52 bar definitely prove that the measured dependence on phase angle is not an artifact of the gas concentration slowly increasing. That is, the same trends are observed after reversing the direction in which the phase angle is changed. The observed differences in SL intensity between runs can be attributed to differences in gas concentration and ambient bubble radius. Indeed, the data in Fig. 2 show a coarse correlation between maximum SL intensity achieved in a given run and age of the water batch used. The older the water, the larger the SL intensity [7]. We were unable to conduct a run that spans a whole cycle of the high frequency, 36° in Fig. 2. This fact might also contribute to differences of the SL intensity between runs. The horizontal lines indicate the single-frequency SL intensity measured immediately before and/or after the double-frequency data. At 0.26 bar there seems to be a phase angle that maximizes the SL intensity. At 0.52 bar there is no definitive indication of *local* minima or maxima. However, this could be partially due to the observed fact that in a neighborhood of the maximum SL emission the bubble changed position very easily when the phase angle was changed. Thus mapping a *local* maximum becomes difficult. The enhancement in SL intensity is 2.75 times for run 1 at 0.26 bar. There is no clear indication as to which of the two amplitudes is more efficient, since changes in gas concentration could be important when comparing two different runs. At higher-frequency amplitudes, it was difficult to keep the bubble in a fixed position for more than a few data points.

Figure 3 shows the bubble radius for different phase angles at 1.50 and 0.26 bar of the low and high pressure, respectively. No clearly noticeable correlation between phase angle and radius change with time can be noticed. The ratio of the maximum to equilibrium radius, R_m/R_e, is a little less than 10 for all cases. The Rayleigh-Plesset equation as

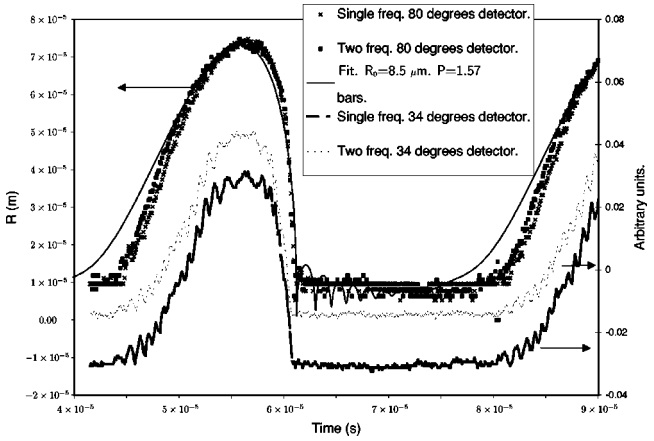

FIG. 4. Bubble radius evolution as measured by two detectors.

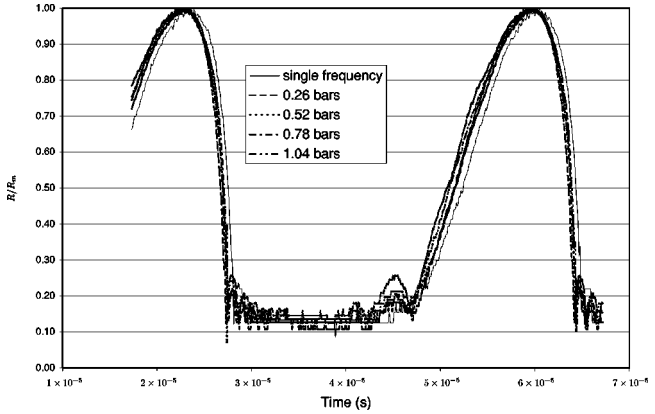

FIG. 5. Normalized bubble radius at $-28.5°$ for different high-frequency amplitudes. Low-frequency pressure amplitude $=1.5$ bars.

implemented in [8] was fit to the single-frequency data in Fig. 3. The ambient radius R_0 and the pressure amplitude P resulting from the fit are 7.00 μm and 1.50 bars, respectively. We believe that the increased SL intensity is due to a decreased minimum radius at the moment of the bubble collapse. Unfortunately, our experimental setup cannot resolve the minimum radius. In order to verify that the maximum radius R_m is independent of the phase angle, the two-detector technique was used. Figure 4 shows the bubble radius evolution as measured by both detectors for single frequency and for the high frequency at 0.26 bar. The single-frequency data from the PMT angled at 80° were used to fit the Rayleigh-Plesset equation, which predicts $R_0=8.50\,\mu$m and $P=1.57$ bars. The output of the APD angled at 34° shows a series of maxima and minima. For both cases, single and two frequencies, the number of maxima observed between the maximum and equilibrium radius is 14. Our Mie theory calculations conducted using the software in [5] predict that the change of radius between two consecutive maxima is 4.84 μm. Therefore the radius change is 14×4.84 μm $=67.76\,\mu$m and the maximum radius is approximately $R_m \approx R_0+67.76\,\mu\text{m}=76.26\,\mu$m. As shown in Fig. 4, this maximum radius is in excellent agreement with the maximum radius predicted by the fit of the Rayleigh-Plesset equation. It is stressed that in Fig. 4 the number of maxima observed and consequently the radius change between equilibrium and maximum radius are the same for single- and double-frequency excitation. Thus the maximum radius does not change by the presence of the high-frequency driving.

Figure 5 shows the bubble radius at constant phase angle for different high-frequency pressure amplitudes. The ratio R_m/R_e takes values similar to those of Fig. 3. A small oscillation is visible just before the bubble starts to expand. Other researchers [3] have found similar radius oscillations for single-frequency excitation. They were unstable and lasted only a few cycles. However, the oscillations we observed were very stable.

Additionally, we found that the presence of the tenth-harmonic frequency component [i.e., even at the lowest achievable pressure amplitudes (at $10f_0$) in our system] can lead to significant enhancements in the stability of the bubble undergoing SL. This allowed the bubble to be driven with pressure amplitudes of 2.0 bars which are far above the often-reported thresholds of 1.4 bars at the fundamental frequency itself, thereby leading to increased levels of SL light emission (by more than 250%). Notably, the maximum drive voltage to the piezoelectric drivers at the fundamental frequency we could attain without the $10f_0$ component was usually about 220 V, after which the bubble became destabilized enough to breakup and dissolve. According to our needle hydrophone calibration, this voltage (220 V) corresponds to 1.4 bar driving pressure amplitude. By merely turning on the high-frequency component (i.e., drive the voltage to the high-frequency piezoelectric drivers at the lowest setting possible of 50 mV from the wave generator), it became possible to increase the drive voltage to the piezoelectric drivers at the f_0 frequency to $\sim$317 V, without losing the bubble. This gave us the ability to increase the driving pressure to $1.4\times317/220=2.0$ bars, which is $\sim$50% higher than the published, often-quoted 1.4-bar barrier well documented in the literature [6,9,10]. We verified that the relationship between voltage and pressure is linear at f_0 in this chamber. The phase diagrams in Ref. [10] indicate that

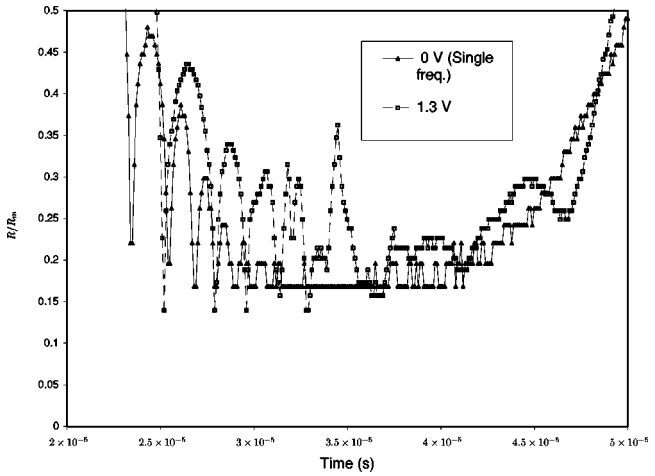

FIG. 6. Rebound region of normalized bubble radius vs time evolution (averaged over eight cycles) for a non-SL bubble driven at $9f_0$ for $-3.9°$ between wave generators. Fundamental frequency pressure amplitude$=0.97$ bars. The voltages in the legend are the rms voltage at the high-frequency piezoceramics. The sharp deformed rebounds produced by the high-frequency excitation should be noted.

stable SL is not possible above 1.5 bars due to after-bounce shape instabilities. Figure 6 shows the rebound regions of the normalized radius versus time evolution for a stable bubble driven with single- and double-frequency excitation schemes, respectively. The high-frequency rebounds from dual-frequency excitation are clearly visible, but are absent for single-frequency excitation. These sharp fluctuations from dual-frequency excitation may be acting to dampen out the after-bounce instabilities described in Ref. [10]. Alternately, the higher-frequency component may be assisting to keep the bubble levitated by trapping it in the high-frequency antinode.

CONCLUSIONS

It has been shown that stable sonoluminescence bubbles can be produced when the fundamental and tenth harmonics are used. Moreover, it was shown that for a fixed bubble position, there is a strong correlation between the SL light emission and the phase angle between harmonics. Adjusting the phase angle, it is possible to enhance the SL emission by as much as a factor of 2.7. No changes of the maximum radius were measured, strongly suggesting that the high-frequency driving produces more violent collapses without affecting the maximum radius. It has also been shown that stable single-bubble SL is possible at pressures as high as 2.0 bars when a small-amplitude high-frequency excitation is used. Since only a small portion of parameter space was explored, it is conceivable that even more intense SL can be achieved. A great advantage of using very high frequencies at small amplitudes is that it is possible to decouple the dynamics of the bubble levitation and of bubble collapse. Thus, not only can one obtain substantial gains in SL intensity and bubble stability, but also studies on bubble instability behavior can be carried out.

[1] J. Holzfuss, M. Ruggeberg, and R. Mettin, Phys. Rev. Lett. **81**, 1961 (1998).

[2] G. Delgadino, Ph.D. thesis, Rensselaer Polytechnic Institute, 1998.

[3] G. Delgadino, F. J. Bonetto, and R. T. Lahey, Jr. (unpublished).

[4] B. P. Barber, R. A. Hiller, R. Lofstedt, S. J. Putterman, and K. R. Weninger, Phys. Rep. **281**, 74 (1999).

[5] P. W. Barber and S. C. Hill, *Light Scattering by Particles: Computational Methods* (World Scientific, Singapore, 1990).

[6] R. G. Holt and F. G. Gaitan, Phys. Rev. Lett. **77**, 3791 (1996).

[7] Most runs were conducted in water that has been in the chamber for more than 1 h, 15 min. Since the measured gas concentration for water that was 1 h, 15 min in the chamber is 27% (at 16 °C), for most runs the expected air concentration was above 27%. Stable single-bubble sonoluminescence has been observed for air concentrations up to 50%. [6]. A typical duration of a run ranged from 30 min to 1 h.

[8] B. P. Barber, Ph.D. thesis, University of California, 1992 (unpublished).

[9] D. F. Gaitan, Ph.D. thesis, University of Mississippi, 1990 (unpublished).

[10] S. Hilgenfeldt, D. Lohse, and M. P. Brenner, Phys. Fluids **8**, 2808 (1996); **9**, 2462(E) (1997).